Scanning Electron Microscopy

Volume 1982
Number 1 *1982*

Article 10

1982

# Monte Carlo Calculations for Electron Microscopy, Microanalysis, and Microlithography

David F. Kyser
*IBM Research Laboratory*

Electron Beam Interactions With Solids (Pp. 119-135)
SEM, Inc., AMF O'Hare (Chicago), IL 60666, U.S.A.

# MONTE CARLO CALCULATIONS FOR ELECTRON MICROSCOPY, MICROANALYSIS, AND MICROLITHOGRAPHY

David F. Kyser *

IBM Research Laboratory
San Jose, California 95193

## Abstract

The methodology of Monte Carlo simulation for electron scattering and energy dissipation in solid targets is reviewed. The basic concepts of single and multiple elastic scattering models are compared, and the continuous energy loss model for inelastic scattering is discussed. Some new developments in Monte Carlo simulation are reviewed, including improvements in the elastic scattering model and discrete models for inelastic scattering. A variety of practical applications of Monte Carlo calculations in the fields of electron microscopy, electron probe microanalysis, and electron beam lithography are reviewed. The Monte Carlo computer program listings available in the literature are also described.

Reprinted from:
SCANNING ELECTRON MICROSCOPY/1981/I
(Pages 47-62,46).
SEM Inc., AMF O'Hare (Chicago), IL 60666, USA

*Present address:
Philips Research Laboratories Sunnyvale
C/O Signetics Corporation
811 E. Arques Avenue
Sunnyvale, CA 94086

KEY WORDS: Monte Carlo, electron scattering, electron energy loss, electron microscopy, electron probe microanalysis, electron beam lithography, elastic electron scattering, inelastic electron scattering.

## I. Introduction

Due to the complex nature of electron-target interactions in solids, a rather large scientific literature has been generated which employs Monte Carlo calculations for predicting the measurable signals from such interactions. A Monte Carlo calculation is simply a theoretical simulation of the three-dimensional trajectory path of the incident primary electron (and any subsequent electron products) as it decelerates within the solid target. The trajectory is actually a series of straight line segments put end-to-end, and the orientation of each segment is determined by the scattering angles associated with the equations used to approximate the physical processes. The term "Monte Carlo" arises from the use of random numbers to select a particular angle (or some other variable) for a particular segment, and hence digital computers are employed to generate the appropriate random numbers and to perform other calculations necessary to describe the trajectory. Because real electron beams are composed of many electrons, a large number of electron trajectories must be simulated within the target since no two electrons will have identical trajectories. Hence, a Monte Carlo calculation is essentially a statistical "experiment", namely a histogram of some signal intensity generated versus some variable of interest with a particular histogram resolution in that variable. The "noise" in the histogram is intimately related to the number of electrons simulated.

The increasing popularity and variety of Monte Carlo calculations in the literature is due to at least 4 factors: (a) the capability to simulate trajectories in complex configurations such as film/substrate targets or small particles, (b) the large variety of signals which can be calculated such as backward and forward scattered electrons with their angular/energy distributions, etc., (c) the "physical" insight and ease of data interpretation obtained, and (d) the ready availability of large digital computers and fast processors. These factors will be described in more detail later.

The main purpose of this paper is to educate the novice in the methodology of Monte Carlo calculations for electron microscopy, microanalysis, and microlithography. Hence, it is tutorial in nature, rather than an original contribution to the art and science of Monte Carlo calculations. A variety of literature is referenced, including some of the original contributions by the author and his colleagues. Because of the large literature encountered, it is

not practical to include all of it. Thus the references reflect those which the author has found most helpful, and are not necessarily all inclusive. In particular, an emphasis is placed on work published within the last 10 years or so. However, we should mention the relevant pioneering work of the past such as Berger [1], Green [2], Bishop [3], Shinoda, Murata, and Shimizu [4], Reimer [5], and Duncumb [6]. These results and successes encouraged many others to adopt and adapt Monte Carlo calculations for a variety of applications and we owe much to their early work.

In addition to these references, there are several groupings of Monte Carlo papers contained in the following sources:

1. NBS Special Publ. 460, ed. by K. Heinrich, D. Newbury, and H. Yakowitz (National Bureau of Standards, 1976).
2. Proc. 8th Int. Congress X-Ray Optics and Microanalysis, ed. by D. Beaman, R. Ogilvie, and D. Wittry (Pendell Publ. Co., 1980).
3. Proc. 6th Int. Congress X-Ray Optics and Microanalysis, ed. by G. Shinoda, K. Kohra, and T. Ichinokawa (Univ. of Tokyo Press, 1971).
4. Microbeam Analysis - 1979, ed. by D. Newbury (San Francisco Press, 1979).

The papers contained in these groupings represent much of the status in Monte Carlo calculation today, and they are highly recommended by the author for education and review.

## II. Basic Concepts in Monte Carlo Simulation

### A. Computer Generation and Utilization of Random Numbers

As mentioned already, a Monte Carlo calculation utilizes computer-generated random numbers to choose particular values for parameters from the distribution of allowed values. However, an electron trajectory is not completely "random", since the random numbers are often utilized within an appropriate function to choose the parameters which describe the trajectory results. There is usually a need for a relatively large number of "random" numbers. These numbers are used in various ways, e.g., to pick a particular value of scattering angle at each scattering point in Fig. 1. The term "uniformly distributed" random numbers refers to the concept that there is equal probability for any particular number to be generated, within a particular interval of numbers. Usually the interval is between 0 and 1. There are many different ways to generate a "uniformly distributed" random number and to test for its randomness. The full treatment of this subject is beyond the scope of this paper. However, one of the most useful methods for Monte Carlo simulation, and one employed in the present work, is that of the congruential method for generating pseudorandom numbers. The details of this method can be found in Hammersley and Handscomb [7] and in Knuth [8]. In such methods, one starts with an "initial" random number which is subsequently utilized in a computer subroutine program to trigger the calculation of a sequence of additional random numbers. The randomness and length of the random number list is controlled by the input parameters in the subroutine. The list of random numbers is subsequently

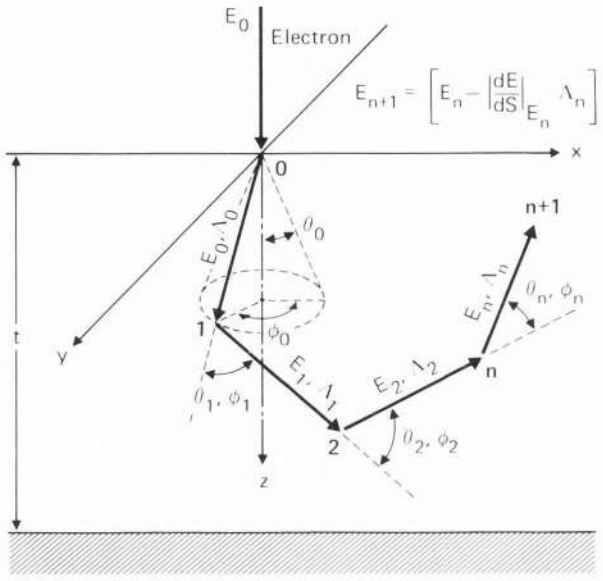


Fig. 1: Geometry of the initial steps of electron scattering and energy loss for a semi-infinite thick target.

used in simulation calculations as described. Interestingly enough, the list of random numbers can be duplicated at will by simply using the same initial random number as the trigger. Hence, Monte Carlo calculations can be repeated exactly if desired, with the identical statistics, etc. Nevertheless, the results of the calculation are still based on randomness and statistics. The point is that with the congruential method, the randomness can be repeated exactly. This appears to be a dichotomy at first, but is only a detail which is of no concern for the present applications. In practice, one lists and divides up the electron trajectories such that a fraction of the total electron trajectories come from only one list. In this way some additional randomness can be incorporated into the calculations. The choice of an "initial" random number is not critical, and any simple convenient scheme can be used such as throwing dice or guessing at a useful sequence of digits to form a number. There are also some types of electronic calculators which can generate a random number upon command.

### B. Concept of Electron Scattering

The trajectory of an electron within a solid target is determined by scattering interactions with the target atoms and their associated electrons. Electron scattering is classified into two types, namely elastic and inelastic. For elastic scattering, the kinetc energy of the scattered electron is the same as that before scattering. This is a good approximation for electron scattering by the atomic nuclei in the target for the energy regime of interest in this paper (1-100kV). For inelastic scattering, there is an abrupt loss of energy by the scattered electron as shown in Fig. 2. This is an approximation used for electron-electron scattering in several versions of Monte Carlo computer programs. In general, both elastic and inelastic scattering processes are operating, and a sophisticated Monte Carlo simulation will attempt to treat them both explicitly and separately. There is also an angular distribution associated

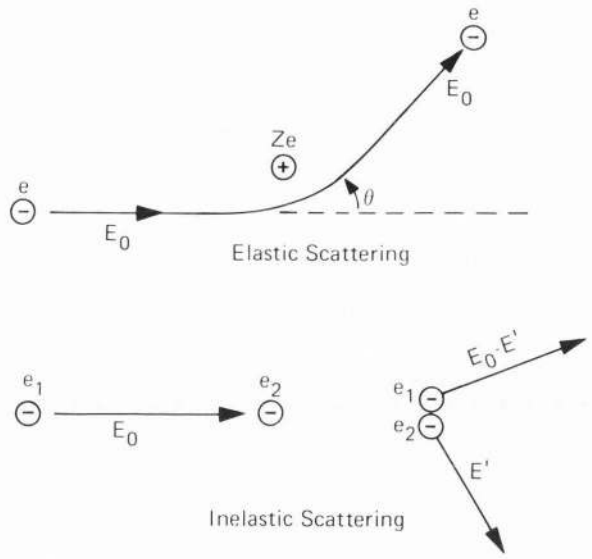


Fig. 2: Elastic electron-atom scattering and inelastic electron-electron scattering schematic.

with each type of scattering, and this distribution is described analytically by a differential scattering cross-section $d\sigma(\theta)=f(\theta)d\Omega$. There may also be more than one type of inelastic scattering process to consider within simulation.

In the case of one mechanism for elastic scattering and one for inelastic scattering, the total cross-section $\sigma_T$ for scattering is simply

$$\sigma_T = \sigma_{el} + \sigma_{inel} \tag{1}$$

where

$$\sigma = \int_{\theta=0}^{\pi} \int_{\phi=0}^{2\pi} \left(\frac{d\sigma}{d\Omega}\right) d\Omega \tag{2}$$

$$= 2\pi \int_{\theta=0}^{\pi} f(\theta) \sin\theta d\theta$$

since the differential solid angle $d\Omega=\sin\theta d\theta d\phi$. Once the electron is scattered (either elasticically or inelastically), then there is a straight-line path assumed to the subsequent scattering point as illustrated in Fig. 1.

In some of the early work on Monte Carlo simulation of electron scattering in solids, a "multiple scattering" approximation was used. In later work, the "single scattering" approximation was preferred to describe the elastic scattering process. These approximations will now be described in more detail.

1. Multiple Scattering

In the multiple scattering approximation, the probability for scattering into the azimuthal angle $\phi$ is uniformly distributed and selected by the relation

$$\phi_i = 2\pi R_i \ (radians) \tag{3}$$

where $R_i$ is a random number between 0 and 1. The probability for scattering into the zenithal angle $\theta$ is often described by a solution of the electron transport equation due to Lewis [9]:

$$f(\theta) = \frac{1}{4\pi} \sum_{\ell=0}^{\infty} (2\ell + 1) P_\ell(\cos\theta) \exp\left(-\int_0^s K_\ell ds\right) \tag{4}$$

where

$$K_\ell = 2\pi N \int_0^\pi f(\theta)[1-P_\ell(\cos\theta)] \sin\theta d\theta \tag{5}$$

and $P_\ell(\cos\theta)$ is the Legendre polynomial. The screened Rutherford cross-section for $f(\theta)$ can be used within Eq. (5), along with the approximation of the exponent as $K_\ell \Delta S$, where $\Delta S$ is the step length between scattering points.

The somewhat arbitrary selection of the step length $\Delta S$ is constrained by opposing factors, as described by Shimizu and Murata [10]. To accurately simulate the electron scattering, small steps are desired. However, to obtain convergence in Eq. (4) large steps are necessary. In addition, large (and equal) steps result in fewer steps per trajectory and hence reduced computer time and cost per simulated trajectory. This advantage of computer efficiency with a multiple scattering model (compared to the single scattering model in the next section) is somewhat negated by the explicit assumption of an infinite medium as a target which is inherently contained within the solution for the transport equation. Nevertheless, the multiple scattering model has been successfully utilized to calculate the properties of backscattered electrons and the depth distribution of X-ray production [e.g., see Ref. 4]. With the decreasing cost of computer calculations, the multiple scattering model has generally been replaced by the more accurate single scattering model which is described next.

2. Single Scattering

In the single scattering model, the step length between scattering points is given by the mean free path

$$\Lambda(cm) = \frac{1}{n\sigma_T} = \frac{A}{N_{Av}\rho\sigma_T} \tag{6}$$

where n is the volume density of the target atoms ($cm^{-3}$), A is the atomic weight (gm/mole) of the scattering atom, and $\rho$ is the mass density ($gm/cm^3$).

For elastic scattering of electrons by the target atoms, the screened Rutherford differential cross-section has often been used [11,12]:

$$f(\theta) = \frac{2\pi Z^2 e^4}{4E^2(1-\cos\theta+2\beta)^2} \tag{7}$$

where E is the kinetic energy of the scattered electron, Z is the atomic number of the scattering atom, and $\beta$ is a screening factor to account for electrostatic screening of the nucleus by orbital electrons. The total cross-section $\sigma_T$ is easily obtained by using Eq. (7) in Eq. (2) to give

$$\sigma_{el}^R = \frac{\pi e^4 Z(Z+1)}{4E^2\beta(\beta+1)} . \tag{8}$$

Note that the factor $Z^2$ in Eq. (7) has been replaced by the factor $Z(Z+1)$ in an attempt to account for inelastic electron-electron scattering with a Rutherford-type cross-section. The limitations of this approximation for

inelastic scattering has been described by Fano [13], and will not be treated here.

The scattering parameter $\beta$ is introduced in Eq. (7) to keep the total cross-section constant. A derivation of $\beta$ for several atomic field functions is described in the appendix of Ref. 4. Typically, an expression where $\beta \propto Z^{2/3}/E$ is used, and very small values of $\beta$ are encountered at the beginning of an electron trajectory. As the electron decelerates and E decreases, then $\beta$ increases. However, since $\beta << 1$, it can be seen that $\sigma \propto (1/E)$ and, hence, $\Lambda \propto E$ (approximately). Thus, in such a "single-scattering" model, the step length gets progressively smaller along the electron trajectory, and the total number of steps per trajectory can be very large compared to that in the multiple scattering model.

As described previously, random numbers are utilized to choose a particular value of $\theta$ from the distribution $f(\theta)$ given in Eq. (7). If $F(\theta)$ is the indefinite integral of $f(\theta)d\Omega$ normalized by the total cross-section $\sigma_T$, then a random number $R_i$ can be used to specify a particular value of $F(\theta)$ and, hence, the scattering angle $\theta$. This concept is illustrated in Fig. 3, and can be used with an analytic description or a numerical description for $f(\theta)$. The indefinite integral of Eq. (7) can be found easily and results in the relation

$$\cos\theta = \left\{1 - \frac{2\beta F(\theta)}{1+\beta - F(\theta)}\right\} \qquad (9)$$

where $F(\theta)=R_i$. The atom specie which scatters the electron in a mixed target is also chosen by another random number, and is based on its fractional cross-section as described in Ref. 12.

C. Concept of Energy Loss

Before going on to describe some of the newer modifications employed in Monte Carlo calculations, we shall describe a popular approximation used for energy dissipation by energetic electrons in targets. To approximate the electron-electron inelastic scattering, which is the dominant mechanism for energy loss, the continuous slowing down formulation of Bethe [14] is often used in the form

$$-\frac{dE}{dS} = \frac{2\pi e^4 nZ}{E}\,\ell n\left(\frac{\gamma E}{J}\right) \qquad (10)$$

where $\gamma=(e/2)^{1/2}$ and J is the mean ionization energy for the target. Conceptually, the electron loses energy at a smooth rate dE/dS (eV/cm) along the path S. Since E is decreasing along S, then -dE/dS increases continuously with decreasing E. Between scattering points in the Monte Carlo simulation, the energy loss is continuous, and hence, the energy at the end of a step length $\Delta S=\Lambda$ depends on both the initial energy E of the scattered electron and the mean free path $\Lambda$. In this way, a full electron trajectory can be simulated by connecting together a series of step lengths and their associated geometry as shown in Fig. 1. However, Eq. (10) cannot be used down to arbitrarily small values of E, but is limited by the log term to the region where $\gamma E/J>1$. Since J/Z is about 10-15eV where Z is the atomic number of the target, then the limit of application also depends on the target. In addition, the approximations used in the derivation of Eq. (10) are less accurate at larger values of Z. Nevertheless, this approximation for energy loss has been used quite successfully within Monte Carlo calculations for a variety of applications.

As an example, we show in Fig. 4, some electron trajectories in Si, Cu, and Au with 90° incidence. These results were obtained with the Monte Carlo program of Kyser and Murata [15] which utilizes Eq. (7) to describe elastic scattering and Eq. (10) to describe energy loss. There is no explicit accounting for inelastic scattering except as described previously. Note that in order to compare the trajectory distribution, a distance scale in units of mass thickness $\rho x$ has been used in order to normalize out the differences in mass density $\rho$. This is allowed because the mean free path $\Lambda$ scales linearly with $\rho$ via Eq. (6). The numerical values of J/Z recommended by Berger and Seltzer [16] were used in Eq. (10). As illustrated in Fig. 4, the onset of a random distribution occurs closer to the surface with Au than for Cu, and for Cu than for Si. This illustrates the strong effect of atomic number Z on electron scattering distributions. In addition, the electron backscatter yield $\eta$ is higher for Au than for Cu and Si. With a tilted surface, the yield $\eta$ also increases. All of these effects are clearly seen in such trajectory plots, and much insight can be gained from them.

Since both the spatial position of each electron and its associated rate of energy loss is calculated, the spatial distribution of energy deposition can be plotted also in the form of equi-energy density ($eV/cm^3$) contours. For the targets shown in Fig. 4, the corresponding contours are shown in Fig. 5. The change in the shape and location of such contours with target Z is apparent. These distributions have subsequent consequences such as spatial resolution in microscopy, microanalysis, and microlithography which will be mentioned later.

D. Sequence of Monte Carlo Calculation

The initial sequence of events in a trajectory simulation is illustrated in Fig. 1. An electron with energy $E_0$ is incident at the origin on a flat target, the x-y plane being the surface. The first scattering event can be at the surface or distributed in some fashion below the surface. The mean free path $\Lambda_0$ for scattering can be calculated via Eq. (6). If both elastic scattering and inelastic scattering are explicitly simulated, then the type of scattering is chosen with a generated random number $R_1$ such that if $R_1 \le \sigma_{e\ell}/\sigma_T$ the scattering is elastic. If $R_1 > \sigma_{e\ell}/\sigma_T$ the scattering is inelastic. The zenithal angle of scattering $\theta_0$ is also chosen with another random number $R_2$ via the distribution such as that shown in Fig. 3. The azimuthal angle of scattering $\phi_0$ is chosen with another random number $R_3$ via Eq. (4). With $\Lambda_0$, $\theta_0$, and $\phi_0$ determined, the spatial position 1 of the next scattering point is determined by trigonometry via directional cosines, and using the incident axis as a reference axis. The electron energy at position 1 is determined by decrementing the energy with respect to its value at position 0 via Eq. (10) where $dS=\Lambda$ and E is the initial energy. At point 1 the sequence is repeated, using $E_1$ to calculate $\Lambda_1$ and $\theta_1$, etc. The sequence is repeated until the electron energy has decreased to some value near to, but greater than, $J/\gamma$. If the electron escapes the surface, the trajectory is terminated and counted as a backscattered electron. Many electrons are simulated in succession to achieve a desired statistical precision in the desired result. The standard deviation of

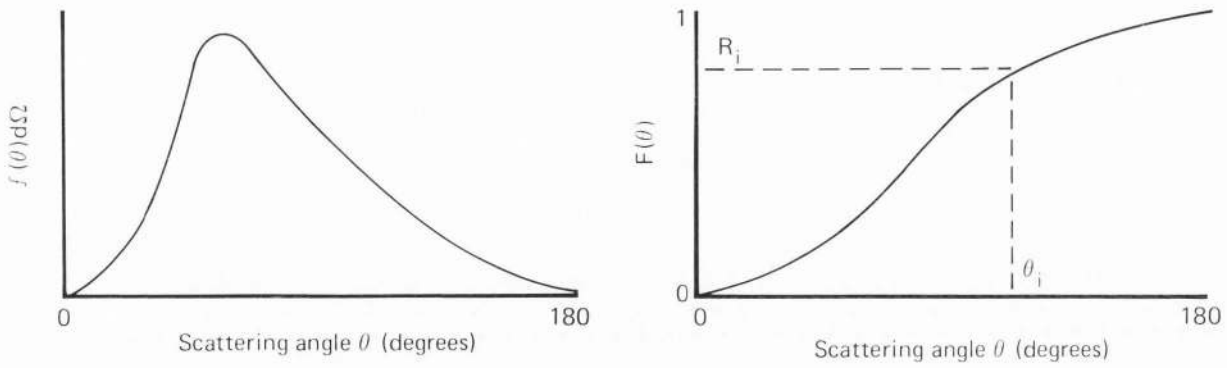


Fig. 3: Selection of scattering angle with indefinite integral of the differential scattering cross-section and a random number.

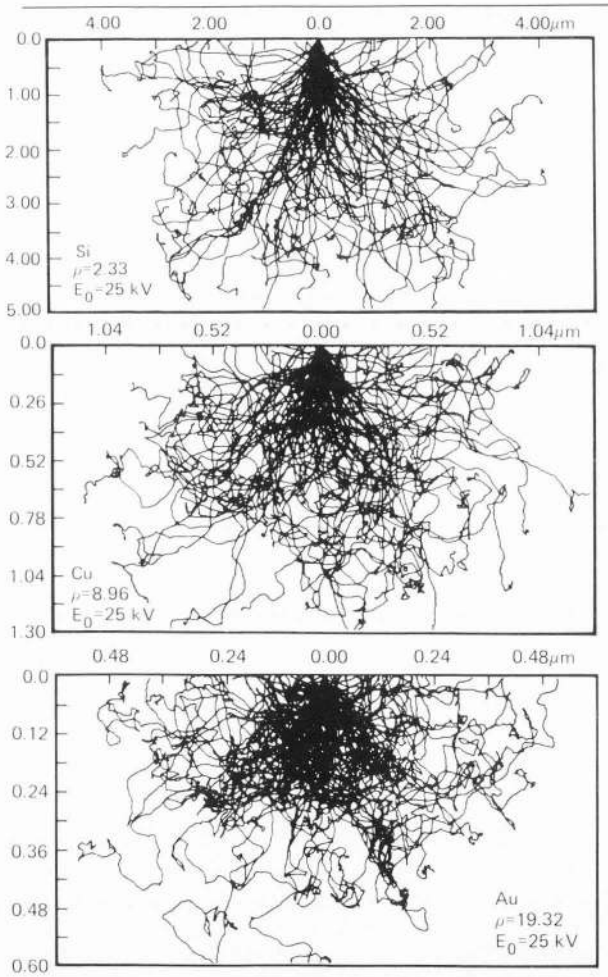


Fig. 4: Projection of 100 electron trajectories in thick targets of (a) Si, (b) Cu, and (c) Au with 25kV energy. The scales are in microns, and have been normalized with the relative mass densities 2.33, 8.96, and 19.32 gm/cm$^3$, respectively.

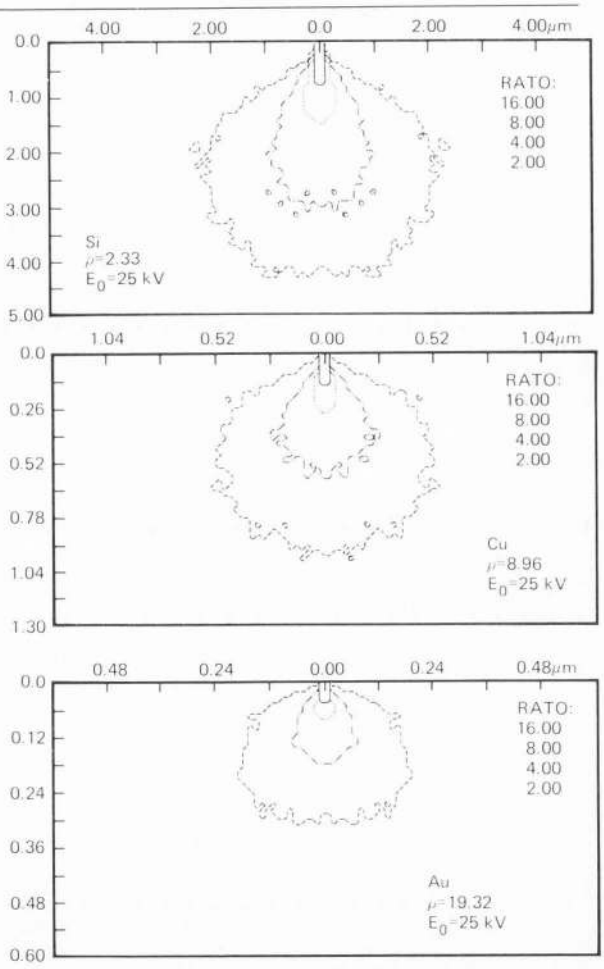


Fig. 5: Equi-energy density contours for the absorbed energy density (eV/cm$^3$) corresponding to Fig. 4. The contour values are relative to the same absolute value in the ratio 16:8:4:2.

the statistical result is given by $\sigma = \sqrt{N}$ where N is the number of trajectories simulated. Hence the relative standard deviation $\sigma_i = \sigma/N = 1/\sqrt{N}$.

For quantitative calculations of characteristic X-ray production in the target, an additional relation must be introduced to describe the ionization rate for a particular atomic level along the electron path. Along the step length ds between scattering points, the electron is assumed to have constant energy E. Then the number of ionizations produced for atomic specie i is $dn_i \propto Q_i(E)ds$ where $Q_i(E)$ is the cross-section for ionization and $dS = \Lambda$. The number of X-ray photons is then $p_i = \omega dn_i$ where $\omega$ is the fluorescent yield. The contribution from all step lengths is summed, as well as that from all electron trajectories. This choice of an analytic expression to describe the cross-section $Q_i(E)$ is still of some concern in quantitative analysis. There are a variety of formulas proposed, and these have been discussed by Powell [17].

## III. Recent Developments in Monte Carlo Models

As expected, the results obtained with Monte Carlo calculations depend on the details of the model used. Usually it is not possible to consider explicitly all of the possible scattering processes individually, especially the inelastic scattering processes. The inclusion of more scattering processes will also increase the computational time, and some compromise is necessary between accuracy and cost. In addition, there may be a lack of theoretical or experimental work to fully simulate particular processes. Hence a variety of approximations are utilized, and the particular combination of processes treated and models utilized varies in the literature of Monte Carlo calculations.

The status of Monte Carlo calculations for microanalysis as of 1975 was presented by Bishop [18]. Two major approximations were identified which needed some improvement, namely (1) The Rutherford scattering cross-section and (2) The Bethe energy loss formula, especially for high Z targets. Krefting and Reimer [19] have utilized the more exact Mott elastic scattering cross-section, coupled with a single scattering model for energy loss, to obtain better agreement with experimental results for backscattered and transmitted electrons. In a later paper, Reimer and Krefting [20] describe their complete model as consisting of the following:

(a) single elastic electron-atom scattering with the exact Mott cross-section for larger angle scattering (>10°) instead of the Rutherford cross-section;

(b) treatment of small angle scattering (<10°) by a mean angular deviation with the Lewis formula for multiple scattering;

(c) single inelastic electron-electron scattering (for secondary electrons >200eV) with a formula due to Gryzinski;

(d) continuous energy loss with the Bethe formula, and subtracting the energy loss due to single inelastic scattering in (c).

In an attempt to remove some of the limitations inherent in the use of the Bethe formula for the mean energy loss, both Henoc and Maurice [21] and Shimizu et al. [22] incorporated a distribution for energy loss about the Bethe mean value. Henoc and Maurice chose to use the Landau theory for statistical energy loss distribution, while Shimizu chose to use an exponential distribution for energy loss:

$$f(\Delta E) = (1/\overline{\Delta E}) \exp(-\Delta E/\overline{\Delta E}) \qquad (11)$$

where $\overline{\Delta E}$ is assumed to be equal to the mean ionization energy J in the Bethe equation for energy loss. The exponential distribution was introduced as a speculation, and provides a distribution of $\Delta E$ about the mean value $\overline{\Delta E}$. The actual value of $\Delta E$ used to calculate the energy loss in an inelastic scattering event is given by

$$\Delta E = -(\overline{\Delta E}) \ell n R \qquad (12)$$

where R is a random number between 0 and 1. This results in the distribution of Eq. (11). The choice of elastic or inelastic scattering is based on the relative cross-sections and a random number as usual, and where

$$\Lambda_{inel} = \overline{\Delta E}/(dE/ds) . \qquad (13)$$

The use of this simple change in the Monte Carlo model provided much better agreement between theory and experiment for the energy distribution of electrons transmitted through thin foils of Al [22]. This was expected since the previous use of an elastic scattering process only, coupled with the continuous energy loss model of Bethe, resulted in finite energy loss of all the electrons transmitted. All the electrons would have travelled at least a distance $\Delta s = t$, the foil thickness, and suffered a minimum energy loss $\Delta E = (dE/ds) \cdot t$ to exit the foil. With the explicit inclusion of an inelastic scattering process as an alternative to elastic scattering, and an associated statistical distribution of energy loss, then some of the electrons could be transmitted with very little energy loss. This behavior was in agreement with experimental measurements on thin foils.

A further improvement in the accuracy of the transmitted electron energy distribution for Al foils was obtained by Shimizu et al. [23] with a more fundamental approach to the simulation of energy loss in the Monte Carlo model. Instead of utilizing the Bethe Eq. (10) to simulate the mean rate of energy loss with path length, they utilized theoretical expressions for the inelastic mean free paths due to scattering of fast electrons by (a) conduction band electrons, (b) L-shell orbital electrons, and (c) plasmon excitations. The elastic scattering is still described by the screened Rutherford cross-section, and random numbers are used to select the type of scattering in the usual manner. The success of this method depends greatly on the availability of good theoretical data for the individual inelastic scattering cross-sections, and hence is somewhat limited for application to a wide variety of targets.

An extension of the fundamental approach in Ref. 23 was made later by Shimizu and Everhart [24] via explicit account for the inelastic scattering by valence band electrons. This extension was made by utilizing the cross-section equation for scattering by atomic core

electrons due to Gryzinski [25] with an empirical mean binding energy $\bar{E}_B$ such that the equation

$$\int_{\bar{E}_B}^{E_0} \Delta E \left| \frac{d\sigma(\Delta E)}{d(\Delta E)} \right|_{\bar{E}_B} d(\Delta E) = \left( \frac{dE}{ds} \right)_{Bethe} - \left( \frac{dE}{ds} \right)_{core} \quad (14)$$

was satisfied. The term in brackets within the integrand is the Gryzinski function, and $\Delta E$ is the energy loss. For Al, a value of $\bar{E}_B = 4eV$ provided such agreement. A more detailed discussion of this extension is contained in the Ph.D. Dissertation of Adesida [26].

In some completely independent work, Green and Lecky [27] have also investigated the transmitted electron energy distribution in Al foils with a "direct" Monte Carlo model which also avoids the use of the Bethe equation for energy loss. For elastic scattering, a Thomas-Fermi model is used to obtain the total cross-section. For inelastic scatttering, both collective (plasmon) and individual excitation of conduction band electrons is tested, as well as core level excitations. While the details of this approach are different from those of Shimizu et al. [23], similar improvements in the agreement with experimental results were also obtained.

Following the work of Krefting and Reimer [19,20], some additional work has been reported by Shimizu et al. [28-31] on the use of the Mott partial wave expansion method (p.w.e.m.) to calculate the elastic scattering cross-section rather than the Rutherford method. The new method for calculation involves numerical procedures, as described by Yamazaki [32]. The partial wave expansion method provides better accuracy for the elastic cross-section, especially in the region of small scattering angle, low energy, and large atomic number. A comparison between the elastic cross-section calculated with the partial wave method and the screened Rutherford method is shown in Fig. 6 for Al and Au. Additional results with the Mott cross-section have been described by Kotera et al. [33] for electron scattering in Au. Again, improved agreement with experimental data is obtained for electron scattering yield and energy distribution.

Further attempts to circumvent the limitations of the Bethe formula for energy loss have been reported by Murata et al. [34,35]. In Ref. 34, the Spencer-Fano [36] equation was utilized to better describe the interaction of an electron near the boundary surface of a semi-infinite target. A comparison of the Bethe and Spencer-Fano results for an organic target is shown in Fig. 7. Note the divergence of the results at the surface where some of the larger inelastic scattering and energy loss process is suppressed in the Spencer-Fano theory. In Ref. 35, as well as in Ref. 33, the equation of Kanaya and Okayama [37] was utilized for energy loss, and some improvement at low energy was observed.

Very recently, Murata et al. [38] utilized the discrete inelastic scattering cross-section of Moller [39] within a Monte Carlo calculation to simulate the production of "fast" secondary electrons explicitly. Elastic scattering with a screened Rutherford formula and energy loss with a modified Bethe formula was retained. The trajectories of both the primary and secondary electrons were calculated, and a typical example for an organic target is shown in Fig. 8. Since most of the "fast" secondary electrons are low kinetic energy, their trajectory lengths are much smaller than the higher energy primaries. However, such

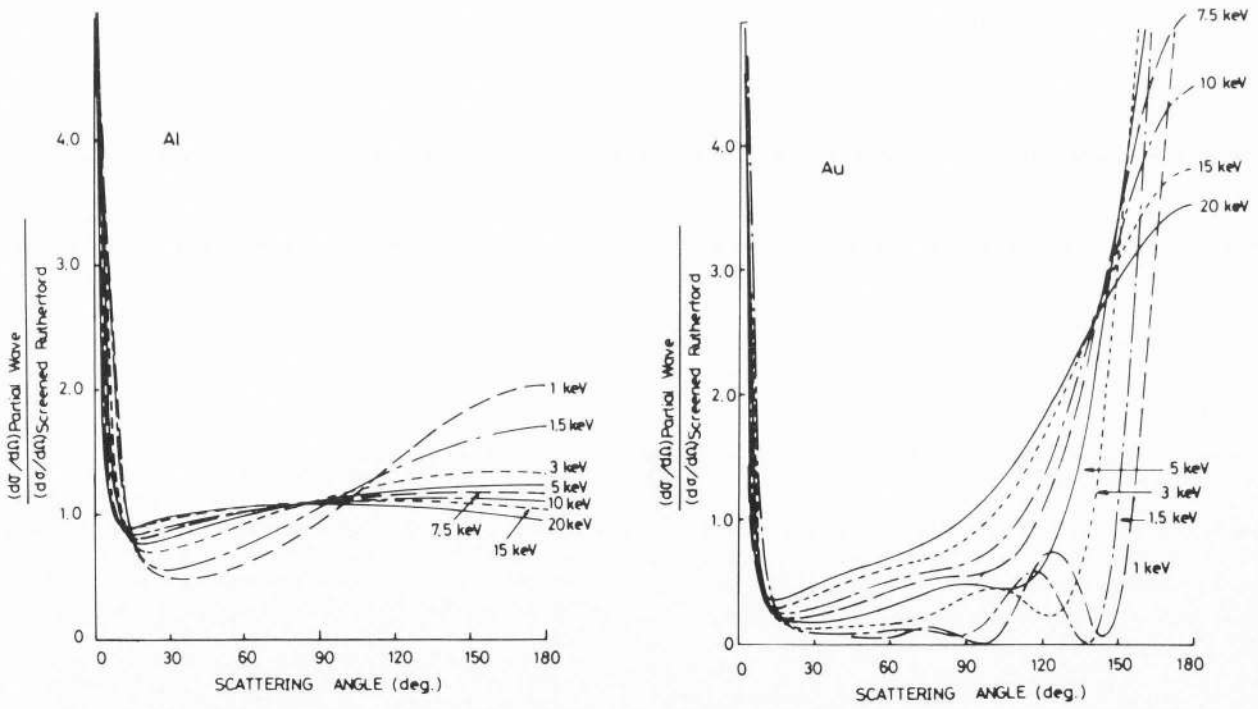


Fig. 6: The ratio of scattering cross-sections obtained by the partial wave expansion method and the screened Rutherford method versus scattering angle for (a) Al and (b) Au (Shimizu et al., Ref. 30).

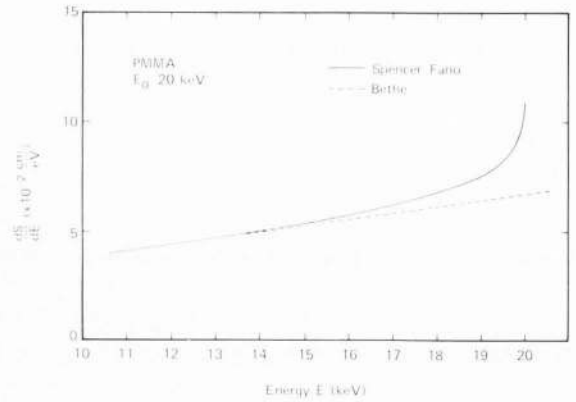


Fig. 7: Comparison of the reciprocal stopping power for PMMA obtained with the theories of Spencer-Fano and Bethe (Murata et al., Ref. 34).

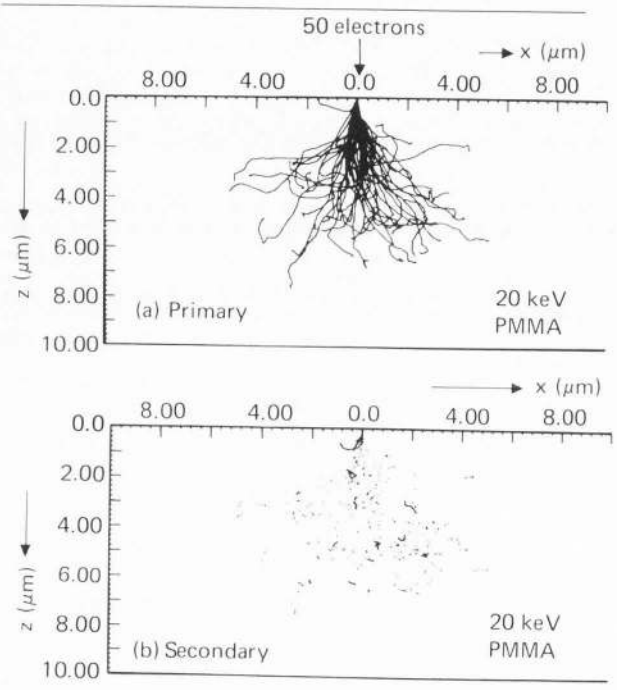


Fig. 8: Projection of electron trajectories for the primary (a) and fast secondary (b) electrons obtained for a thick PMMA target (Murata et al., Ref. 38).

secondaries can be very effective in radiation chemistry processes such as electron beam lithography. The ultimate spatial resolution is determined by such secondary electrons, and this will be described later in more detail.

Lastly, a hybrid Monte Carlo calculation procedure for electron trajectory simulation has been described by Newbury et al. [40]. These authors developed a Monte Carlo program which incorporates both single and multiple elastic scattering. Single scattering is used for the initial 5% of the energy loss, and multiple scattering for the balance of the trajectory. Energy loss is simulated by discrete inelastic scattering during the single scattering portion of the trajectory and continuous energy loss during multiple scattering. This hybrid program combines the advantage of the rapid calculation time of the multiple scattering model with the better accuracy of the single scattering model for the description of electron and X-ray signals.

## IV. Some Practical Applications of Monte Carlo Calculation

Since the Monte Carlo approach to electron trajectory simulation involves the fundamentals of electron scattering and energy loss, it should not be surprising that there is a corresponding variety of practical applications. On the one hand, some of the research has been directed towards improving the fundamental input to the simulation process such as that described earlier. On the other hand, an ever increasing quantity of literature has described numerous applications in the general fields of microscopy, microanalysis, and microlithography. In fact, it appears that much of the Monte Carlo literature in recent years has been centered around the very practical field of electron beam lithography, and this will be discussed more in a later section.

The variety of applications which had been treated with Monte Carlo calculations of electron beam signals was reviewed in an excellent paper by Newbury and Yakowitz [41]. Another good review was also presented by Shimizu [42]. These references describe the applications up to about 1975 or so. In particular, the following applications were described:

1. extent of the primary electron interaction volume
2. lateral and depth distributions of backscattered electrons
3. angular and energy distributions of backscattered electrons
4. lateral and depth distributions of secondary electrons
5. angular and energy distributions of secondary electrons
6. extent of X-ray generation volume
7. depth distribution of X-ray production.

Hence, in this section we will only discuss some newer applications of Monte Carlo calculations which have been described within the past 5 years or so. The author has arbitrarily chosen to put these into 3 categories; namely, (a) microscopy, (b) microanalysis, and (c) microlithography.

### A. Microscopy

One particularly interesting application of Monte Carlo calculations is that of Type II magnetic contrast. This contrast mechanism is due to the Lorentz force applied to an electron travelling in a magnetic field or magnetized material. The direction of the force depends on the relative directions of the electron velocity v, and the magnetic field B. The magnitude of the force $\overline{F} = e(\overline{v} \times \overline{B})$ acting over a time $t = \Lambda/v$ for each mean free path length will perturb the electron trajectory and modulate the electron backscatter yield. The yield will be modulated as shown qualitatively in Fig. 9. Following the original work of Newbury et al. [43] and Ikuta and Shimizu [44], some

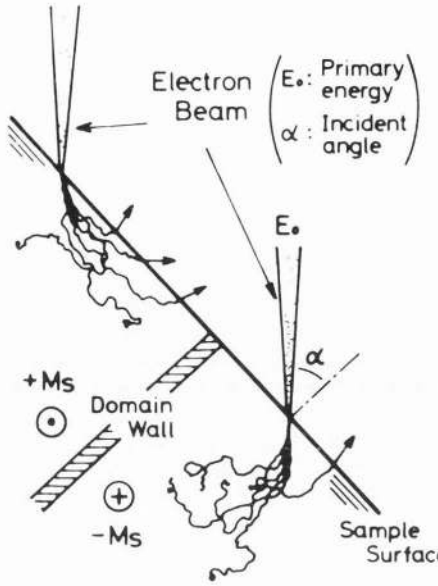


Fig. 9: Schematic illustration of the perturbed electron trajectories within a magnetic material with saturation magnetization $M_s$ (Ikuta et al., Ref. 45).

additional work has been presented by Ikuta et al. [45]. These new calculations show how the spatial resolution of Type II magnetic microscopy changes with (a) incident beam velocity and (b) detection angle. Some examples of their results are shown in Fig. 10. The authors concluded that (a) spatial resolution decreases with increasing beam voltage and (b) spatial resolution increases with detection of the low-loss electrons only, i.e., the forward-scattered electrons.

Another interesting application of Monte Carlo calculations is that for predicting the spatial resolution in analytical electron microscopy (AEM) of their foils with X-ray microanalysis. Following the original work by Kyser and Geiss [46], additional results were presented by Newbury and Myklebust [47], Geiss and Kyser [48], and Kyser [49]. With such thin foils ($\leq 0.2\mu m$) and high beam voltages ($\geq 100kV$) the volume of X-ray production is very small, as illustrated in Fig. 11. Monte Carlo calculations are very advantageous for this application since very little computer time per trajectory is required, and hence a large

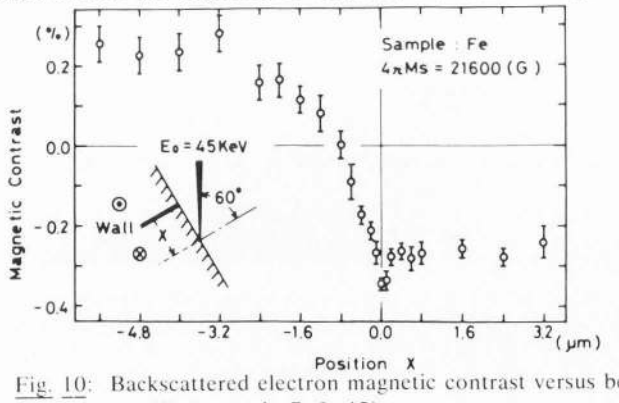


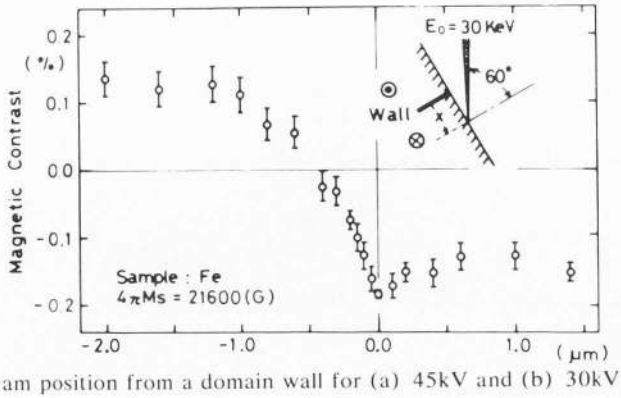


Fig. 10: Backscattered electron magnetic contrast versus beam position from a domain wall for (a) 45kV and (b) 30kV beam energy (Ikuta et al., Ref. 45).

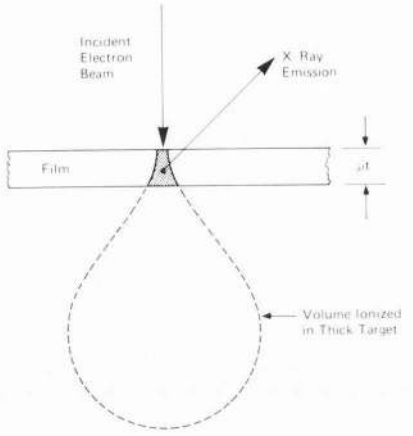


Fig. 11: A qualitative display of the volume analyzed in a foil, relative to that in a thick target (Kyser, Ref. 49).

number of trajectories can be calculated easily for high statistical precision. In addition to the characteristic X-ray production, the continuum X-ray production can also be calculated [48]. These results show that the peak to background ratio (P/B) increases with increasing beam voltage $E_0$. With regard to spatial resolution for microanalysis in AEM, some results obtained by the author for Cu foils are shown in Fig. 12. Note that even for a vanishingly small electron beam diameter, there is still a limited spatial resolution due to forward electron scattering

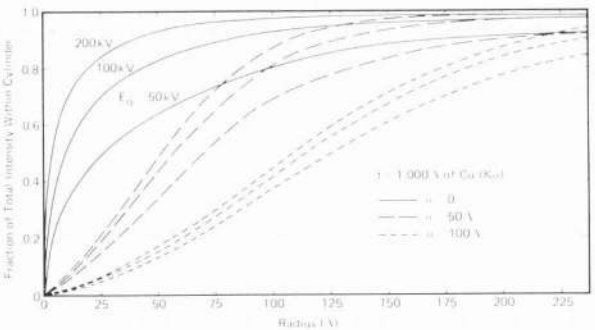


Fig. 12: Composite of Monte Carlo results for 0.1 micron foils of Cu at various beam voltages and Gaussian beam diameters (Kyser, Ref. 49).

in the foil. The resolution expected for a variety of foil materials and thicknesses at $E_0$=100kV is given in Table 1. Note that resolution degrades with increasing atomic number and foil thickness. Further insight into spatial resolution can be obtained by simply plotting electron trajectories, such as those shown in Figs. 13 and 14 for Cu and Au foils with normal and 45° beam incidence.

In such calculations of spatial resolution, the Monte Carlo model has some unique advantages relative to alternative models:

1. any foil thickness can be treated
2. any beam distribution incident can be simulated
3. any beam angle incident can be simulated
4. any X-ray take-off angle can be treated
5. X-ray absorption correction included
6. any multi-element target can be treated
7. atomic number effects on X-ray production included.

TABLE 1

Summary of Monte Carlo calculations defining the cylinder diameter d(Å) which contains 90% of the total X-ray production within the foil for $E_0$=100 keV, $\sigma$=0. The values in parenthesis are for $\sigma$=50Å.

| Film Material and X-ray | Film Thickness (Å) | | | |
|---|---|---|---|---|
| | 400 | 1000 | 2000 | 4000 |
| C (Kα) | --- ---- | 50 (200) | 130 (230) | 250 (300) |
| Al (Kα) | 20 (195) | 90 (220) | 200 (250) | 460 (460) |
| Cu (Kα) | 40 (205) | 160 (250) | 550 (550) | 1400 (1400) |
| Au (Lα) | 80 (220) | 380 (400) | 1300 (1300) | 4500 (4500) |

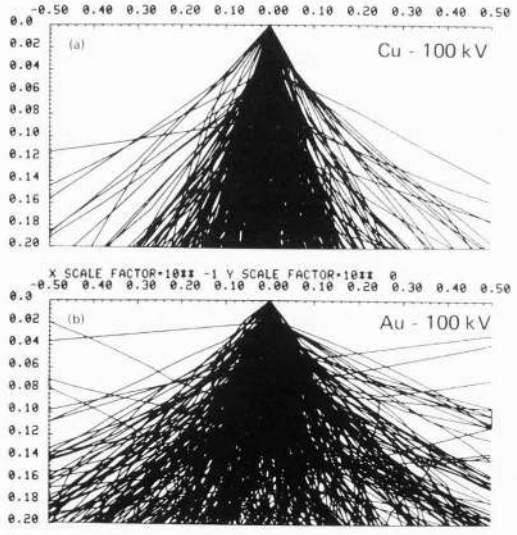


Fig. 13: Projection of 400 electron trajectories in 0.2 micron foils of (a) Cu and (b) Au for a 100kV point source beam, normal incidence. The vertical and lateral scales are in microns, but unequal by 4X (Kyser, Ref. 49).

B. Microanalysis

Monte Carlo calculations have been utilized for quantitative chemical microanalysis of particles, thin films, and bulk samples. For particle analysis, theoretical calibration curves of X-ray production versus particle diameter have been generated for particles of known composition [50,51]. However, due to the complex procedures required for the analysis of unknown particles, it is recommended that Monte Carlo calculations be used mainly to guide and test the design of more simple methods for analysis.

Following the original work of Kyser and Murata [15] for electron probe microanalysis of alloy films on thick substrates, there has been additional work described. Utilizing the Monte Carlo program of Ref. 15, Cvikevitch and Pihl [52,53,54] have extended the applications to refractory thin films of Ta-W and Ti-W on silicon [52], films of Sn-O and Pb-O on Pb and Sn [53], and films of Au-Pd-Cu [54]. These authors have demonstrated that Monte Carlo calculations are very practical for thin film analysis, and have also shown that the data analysis can be accomplished with relatively few trajectories simulated for each case in the calibration curves. This work has also established such Monte Carlo calculations for practical thin film analysis as the only nondestructive technique for true microanalysis, i.e., quantitative analysis of small areas. With increasing availability of Monte Carlo programs, this technique will become more widespread in the microanalysis community. Additional work on thin film analysis with Monte Carlo calculations has been described by Murata et al. [35].

For quantitative microanalysis of both the film composition and film thickness, the Monte Carlo model is utilized to generate theoretical calibration curves of intensity ratio $k_i$ versus weight fraction $C_i$ with mass thickness $\rho t$ as a parameter. An example of such a

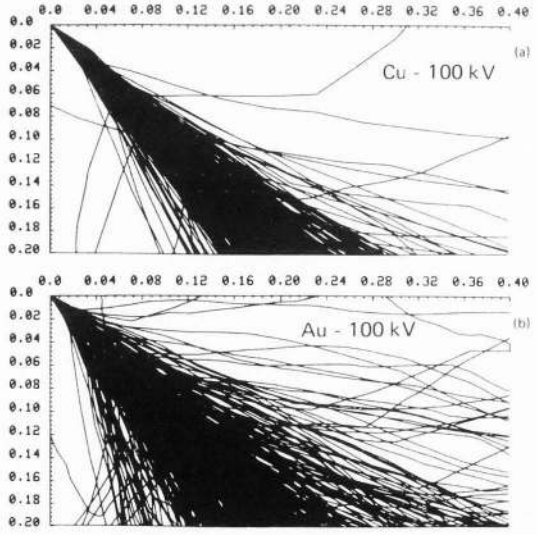


Fig. 14: Projection of 400 electron trajectories in 0.2 micron foils of (a) Cu and (b) Au for a 100kV point source beam, 45° incidence. The scales are in microns, and are equal for vertical and lateral directions (Kyser, Ref. 49).

calibration curve is shown in Fig. 15 for a Mn-Bi alloy film on $SiO_2$ substrate. As described in Ref. 15, the exprimental $k_i$ are iterated within these calibration curves to converge on a unique solution for $C_i$ and $\rho t$. This convergence can be accomplished graphically as shown in Fig. 16. The technique can also be applied to ternary films.

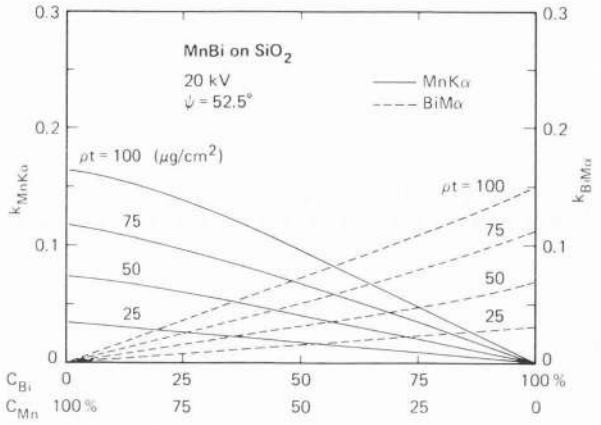


Fig. 15: Monte Carlo-generated calibration curves for Mn and Bi X-ray production in thin Mn-Bi films on $SiO_2$ substrates (Kyser and Murata, Ref. 15).

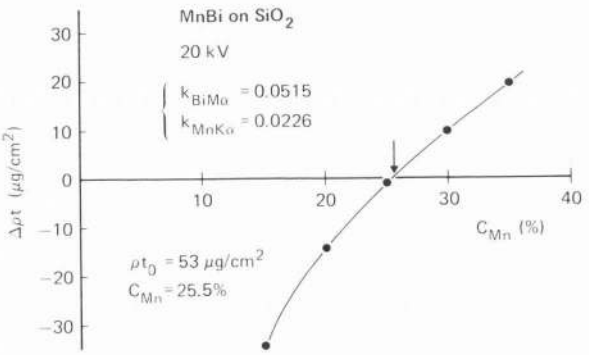


Fig. 16: Graphical convergence of experimental data k from Mn-Bi film within the calibration curves of Fig. 15 (Kyser and Murata, Ref. 15).

When the film composition is known, or in the case of a single element film, the Monte Carlo calculation of X-ray production can be utilized to generate theoretical calibration curves of $k_i$ versus beam voltage $E_0$ and film thickness $\rho t$. Very careful experimental measurements with well-characterized samples were utilized by Reuter et al. [55] and excellent agreement with Monte Carlo calculations were obtained. An example of the agreement for Al films on Si is shown in Fig. 17.

For quantitative electron probe microanalysis of bulk samples, Love et al. [56,57,58] have utilized the simplified Monte Carlo program of Duncumb [6] to generate improved correction for matrix effects. In Ref. 56, the Monte Carlo model was utilized to generate the depth distribution of X-ray production $\phi(\rho z)$ for a wide range of analytical conditions. Based on this theoretical data, an analytic expression for the mean depth was

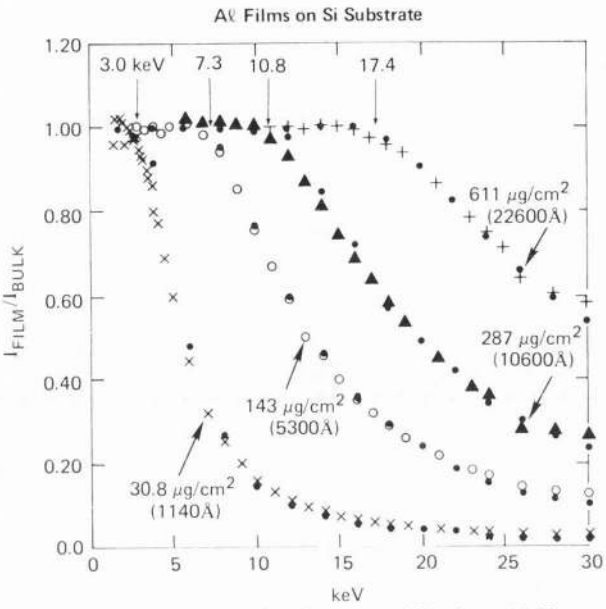


Fig. 17: Normalized Al(Kα) measured for four Al films on Si substrate versus beam voltage. The solid circles are the Monte Carlo results for the same film thickness (Reuter et al., Ref. 55).

deduced and compared with a previous expression. The new form gives the correct dependence on electron energy, while the older form did not. In Ref. 57, the Monte Carlo results were utilized to deduce an improved expression for the atomic number correction in quantitative electron probe microanalysis. Lastly, Ref. 58 described the behavior of the surface ionization function $\phi(0)$ as deduced with Monte Carlo calculations. These papers show the powerful use of Monte Carlo results as a theoretical guide to improvements in the accuracy of quantitative microanalysis via analytic expressions. Hence, the benefits can be realized by a wider community of analysts.

Very recently, Ichimura et al. [31] have demonstrated capability for quantitative Auger electron microanalysis with Monte Carlo calculations. The Monte Carlo calculations provide the quantitative correction necessary for the Auger electron production due to backscattered electrons.

## C. Microlithography

As mentioned previously, many of the practical applications of Monte Carlo calculations have been made in the field of electron beam lithography. In such microlithography, a very thin film (~1μm) of polymeric material is spun onto the surface of a substrate which is to be pattern exposed by a scanning electron beam. Due to the interaction of the electrons with the film, the solubility or etch rate of the film is modified and the pattern exposed by the beam can be developed in the film. The substrate material can then be subsequently patterned through this resist film mask by processes such as chemical etching, ion milling, etc., used in VLSI technology.

Since the density of the polymeric resists utilized are typically low (~1gm/cm$^3$) the high-energy primary electrons (~20kV) easily penetrate into the substrate. Spatial

resolution of the exposure is determined by both the forward scattering of the electrons and by backscattering from the substrate. Such electron scattering and energy loss also leads to "proximity" effects in electron beam lithography (EBL), and Monte Carlo calculations have proven to be very useful in understanding and calculating the magnitude of the proximity effect. The Monte Carlo model is able to deal quantitatively with the discontinuous material boundary between the film and substrate, and without having to segment the problem into two separate models, i.e., one model for forward and another for backward scattering. Within the Monte Carlo model, there is no such separation and electron scattering is calculated with the same model regardless of the scattering direction.

In some early work, both Kyser and Murata [59] and Hawryluk et al. [60] utilized Monte Carlo calculations for the spatial distribution of energy deposited by an electron beam into a thin polymer on a Si substrate. Both of these papers utilized the single scattering model discussed previously. An example of the radial distribution of energy deposition by a point source beam is shown in Fig. 18. This type of distribution has been approximated by a superposition of two concentric Gaussian distributions, with appropriate values for the standard deviation $\beta_i$ and relative areas $\eta$. This Gaussian approximation is often called a "proximity function", and is written in the following form:

$$f(r) = k\left[ \exp(-r/\beta_f)^2 + \eta(\beta_f/\beta_b)^2 \exp(-r/\beta_b)^2 \right] . \quad (15)$$

This form can then be utilized in a comptuer program such as "SPECTRE" [61] to calculate the electron exposure modulation necessary to compensate for proximity effects in EBL. Monte Carlo calculations of f(r) like Fig. 18 have been made by Parikh and Kyser [62] for a variety of cases, and some typical results are shown in Table 2 for the Gaussian parameters of Eq. (15) derived by a least-squares fit to the Monte Carlo distribution. Such Monte Carlo calculations have also been utilized by Kyser and Pyle [63] for the description of the latent image produced by electron exposure of thin films, and the subsequent time-evolution of the developed pattern by a solvent. An example of the dose compensation factor predicted for a 1$\mu$m film of PMMA on Si substrate is shown in Fig. 19 (from Ref. 65).

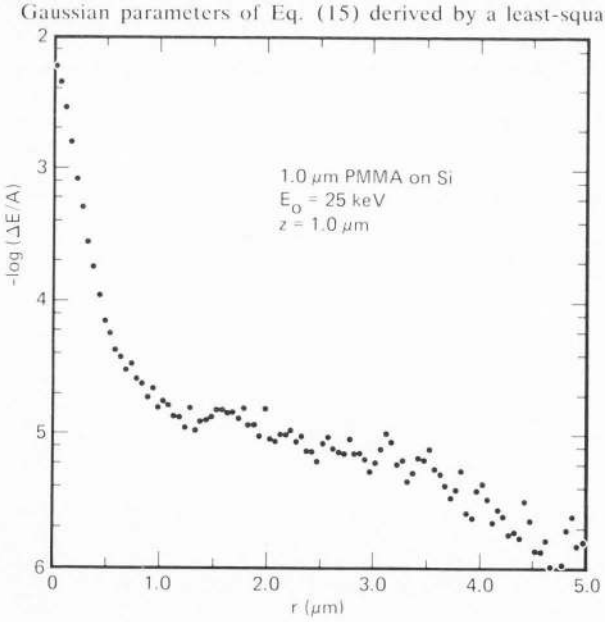


Fig. 18: Radial distribution of the energy deposited in a 1 micron PMMA film on Si substrate by a 25kV beam. The constant $A=(8/\pi)\times10^{18}$ eV/cm$^3$/electron (Parikh and Kyser, Ref. 62).

TABLE 2

Compendium of the three parameters that define f(r) for PMMA-Si. (Note: All parameters are evaluated at z=t)

| $E_0$ (keV) | t ($\mu$m) | $\beta_f$ ($\mu$m) | $\eta_E$ | $\beta_b$ ($\mu$m) | R ($\mu$m) | $\beta_b$/R |
|---|---|---|---|---|---|---|
| 10 | 0.5 | 0.22 | 0.51 | 0.65 | 1.58 | 0.41 |
| 15 | 0.5 | 0.13 | 0.51 | 1.14 | | |
| 15 | 1.0 | 0.44 | 0.52 | 1.41 | 3.12 | 0.45 |
| 25 | 0.5 | 0.06 | 0.51 | 2.6 | | |
| 25 | 1.0 | 0.22 | 0.49 | 2.9 | 7.36 | 0.39 |
| 15 | 1.5 | 0.43 | 0.52 | 2.9 | | |
| 40 | 0.5 | 0.04 | 0.42 | 6.0 | | |
| 40 | 1.0 | 0.11 | 0.45 | 6.0 | 16.22 | 0.37 |
| 40 | 1.5 | 0.22 | 0.44 | 6.2 | | |

Because of the vast literature in the field of EBL, it is not possible to reference all of it which pertains to simulation calculations, including Monte Carlo calculations. The interested reader will find most of the references in the recent Doctoral Theses of Adesida [26], Lin [64], and Stephani [66] who have utilized Monte Carlo calculations for electron trajectory simulation. In addition, the recent papers of Adesida et al. [67,68] should be of interest.

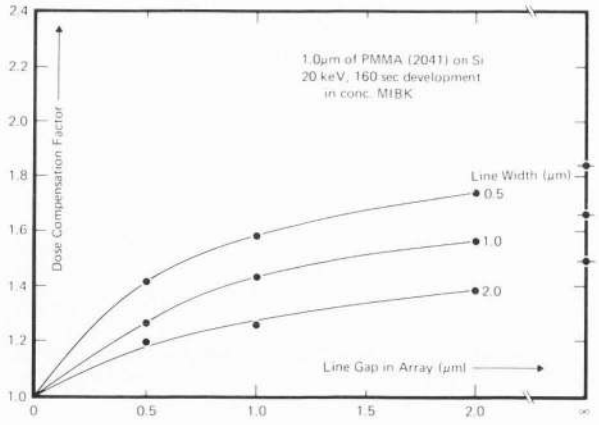


Fig. 19: Dose compensation factor for various linewidths and gapwidths predicted by simulation of developed profiles in PMMA (Neureuther et al., Ref. 65).

## V. Input/Output of Monte Carlo Programs

### A. Computer Programs Available

Due to the variety of approaches, there is not a unique computer program for Monte Carlo simulation of electron scattering and energy loss in solid targets. A brief history of approaches taken before 1975 was given by Bishop [18]. Because a detailed listing of each computer program and its associated input/output is not appropriate here, we will instead refer to those programs which have been published in the literature. A simple program, including a detailed explanation of its use, is contained in Curgenven and Duncumb [6]. A somewhat more sophisticated program is contained in the appendix of Shimizu [69]. A very detailed report, including the computer code and some examples, is contained in Henoc and Maurice [21]. A program for microlithography applications is contained in Hawryluk [70] and also in Lin [64]. Based on the information in these five sources, along with Murata et al. [11,12], anyone with access to a computer facility should easily be able to implement a Monte Carlo program.

### B. Computational Time and Its Control

One common objection to Monte Carlo calculations is their alleged high cost due to long computations on a digital computer. However, the actual cost is completely within the control of the user, and is primarily determined by the model used, the target configuration, and the number of electrons simulated N. For simple calculations, the model of Curgenven and Duncumb [6] can be used. As described previously, the foil application is more economical than the bulk application. Finally, the desired statistical certainty sets the value for N. Since Monte Carlo calculations are not meant to be used for rapid on-line analysis or control, there can be a reasonable time delay between program submission to a computer and the output calculations. Many programs can wait until low-load computer times to be run. For debugging a program, only a few trajectories need to be simulated to check the operation and output calculations for reliability. A high-precision Monte Carlo program should only be run after establishing its reliability. The output of any Monte Carlo calculation can be saved for subsequent use in other applications. However, one must then decide in advance the output variety desired and anticipate the need.

### C. Condensation and Output of Results

The variety of output data available from a Monte Carlo simulation of electron trajectories and energy loss is quite large. It includes the following:

1. electron trajectories plotted for qualitative distribution
2. backward scattered and forward scattered electron yield
3. backward scattered and forward scattered energy distribution
4. backward scattered and forward scattered angular distribution
5. spatial distribution of energy deposition
6. spatial distribution of X-ray production.

Of course, the quantitative accuracy of such calculations depends intimately on the accuracy of the physical model employed. This is true of any model, and the Monte Carlo method does not avoid this necessity. However, the Monte Carlo model is a very intuitive and easy model to simulate physical processes with, once the output desired is identified. The angular, energy, and number yield of backward scattered electrons from foil targets is of some interest, and has been discussed recently by Niedrig [71]. The spatial distribution of energy deposition and its relevance to electron beam lithography has been discussed by Kyser and Viswanathan [72]. The value of Monte Carlo calculations for spatial resolution and quantitative microanalysis has already been discussed. In cases 5 and 6, the output histogram can be in 1, 2, or 3 dimensions as desired. The Monte Carlo model is not limited to flat surfaces or homogeneous targets. Specific boundary conditions on the target can easily be accommodated and incorporated. In some cases, just a simple graphical plot of the electron trajectories will suffice to provide some qualitative or semi-quantitative information.

### D. Monte Carlo Simulation of Ion Beams

In addition to the work on Monte Carlo simulation of electron beam interactions, there is also some considerable results published for ion beam interactions in solids. Although it is beyond the intent of this paper to review such work, the interested reader will find the following references useful. Utilizing the single scattering model, Ishitani et al. [73,74,75] have calculated the ion range, ion backscatter yield, energy distribution of ions transmitted through a thin foil, and depth resolution in SIMS due to atomic mixing. More recently Kang et al. [76,77] have utilized Monte Carlo methods to calculate the sputter yield of Si with $Ar^+$ ions and the depth resolution in SIMS profiling. An alternative approach to Monte Carlo simulation of energetic ions in amorphous targets has recently been published by Biersack and Haggmark [78]. Their Monte Carlo program was developed for determination of ion range and damage distributions with depth, as well as angular and energy distributions of backscattered and transmitted ions. Their computer program provides particularly high computer efficiency, while maintaining a high degree of accuracy.

## VI. Summary

Monte Carlo simulation of electron scattering and energy loss is a very powerful tool for both qualitative and quantitative design and interpretation of experiments. The accuracy of a Monte Carlo calculation is dependent on the accuracy of the physical approximations used in its design, and there is a continuing research effort to identify the areas which need better approximation. However, the Monte Carlo method is a very "physical" one in which the basic concepts are easily grasped and interpreted, and there is a wealth of output available in the form of electron energy, angular, and number distributions for adsorbed, backscattered, and transmitted electrons.

Several versions of a Monte Carlo program are available in the literature, and the serious user is encouraged to start a project on Monte Carlo simulation and tailor it to the application desired. Many applications demand a good model for interpretation and experimental design, and Monte Carlo methods are probably the most flexible and

adaptable, especially for quantitative interpretation. The technical insight and subsequent rewards to be gained are very worthwhile.

## VII. Acknowledgments

The author gratefully thanks Dr. Kenji Murata (Osaka Prefecture University, Japan) for assistance in preparing a Monte Carlo computer program for simulation of electron scattering in solid targets and Mr. Richard Pyle (IBM Systems Product Division) for providing the computer software support for interactive computer graphics.

## VIII. References

1. Berger, M. J. "Monte Carlo Calculations of the Penetration and Diffusion of Fast Charged Particles," in: Methods in Computational Physics, Vol 1, ed. by B. Alder, S. Fernbach, and M. Rotenberg, Academic Press, New York, 1963, 135-213.
2. Green, M. "The Efficiency of Production of Characteristic X-Radiation," Ph.D. Thesis, University of Cambridge, 1962.
3. Bishop, H. E. "Electron Scattering and X-Ray Production," Ph.D. Thesis, University of Cambridge, 1966.
4. Shinoda, G., Murata, K., and Shimizu, R. "Scattering of Electrons in Metallic Targets," in: Quantitative Electron Probe Microanalysis, ed. by K. F. J. Heinrich, National Bureau of Standards, Spec. Publ. 298, Washington, D.C. 20234, 1968, 155-187.
5. Reimer, L. "Monte Carlo Rechnungen zur Elektronendiffusion," Optik 27, 1968, 86-98.
6. Duncumb, P. "Quantitative Electron Probe Microanalysis," in: Proc. 25th Ann. Mtg. of EMAG, The Institute of Physics, London, 1971, 132-137; also see "Simulation of Electron Trajectories by a Simple Monte Carlo Technique," TI Res. Lab. Report 303, 1971 by L. Curgenven and P. Duncumb.
7. Hammersley, J. M. and Handscomb, D. C. Monte Carlo Methods, Methuen and Co., London, 1964, Ch. 3.
8. Knuth, D. E. The Art of Computer Programming, Vol. 2, Addison-Wesley, New York, 1969, Ch. 3.
9. Lewis, H. W. "Multiple Scattering in an Infinite Medium," Phys. Rev. 78, 1950, 526-529.
10. Shimizu, R. and Murata, K. "Monte Carlo Calculations of Electron-Sample Interaction in the SEM," J. Appl. Phys. 42, 1971, 387-394.
11. Murata, K., Matsukawa, T., and Shimizu, R. "Monte Carlo Calculations on Electron Scattering in a Solid Target," Jap. J. Appl. Phys. 10, 1971, 678-686.
12. Murata, K., Matsukawa, T., and Shimizu, R. "Application of Monte Carlo Calculations Based on the Single Scattering Model," in: Proc. 6th Int. Conf. X-Ray Optics and Microanalysis, ed. by G. Shinoda, K. Kohra, and T. Ichinokawa, Univ. of Tokyo Press, 1972, 105-112.
13. Fano, U. "Inelastic Collisions and the Moliere Theory of Multiple Scattering," Phys. Rev. 93, 1954, 117-120.
14. Bethe, H. A. and Ashkin, J. Experimental Nuclear Physics, Vol. 1, ed. by E. Segre, Wiley, New York, 1953, 166-357.
15. Kyser, D. F. and Murata, K. "Quantitative Electron Microprobe Analysis of Thin Films on Substrate," IBM J. Res. Develop. 18, 1974, 352-363.
16. Berger, M. J. and Seltzer, S. M. "Tables of Energy Losses and Ranges of Electrons and Positrons," in: Studies in Penetration of Charged Particles in Matter, Nat. Acad. Sci. Publ. 1133, Washington, D.C., 1964, Ch. 10.
17. Powell, C. J., "Evaluation of Formulas for Inner Shell Ionization Cross-Sections," in: Use of Monte Carlo Calculations in EPMA and SEM, National Bureau of Standards, Spec. Publ. 460, Washington, D.C. 20234, 1976, 97-104.
18. Bishop, H. E. Ibid., 5-14.
19. Krefting, E. R. and Reimer, L. "Monte Carlo Rechnungen zur Elektronendiffusion," in: Quantitative Analysis with EPMA and SIMS, ed. by E. Preuss, Zentralbibliothek, KFA Julich, West Germany, 1973, 114-148.
20. Reimer, L. and Krefting, E. R. "The Effect of Scattering Models on the Results of Monte Carlo Calculations," in: Ref. 17, 45-60.
21. Henoc, J. and Maurice, F. "Application de la Methode de Monte Carlo a la Simulation des Trajectoires des Electrons de 10 a 30keV," CEA Report R-4615, Atomic Energy Commission, France, 1975.
22. Shimizu, R., Kataoka, Y., Matsukawa, T., Ikuata, T., Murata, K., and Hashimoto, H. "Energy Distribution Measurement of Transmitted Electrons and Monte Carlo Simulation for Kilovolt Electrons," J. Phys. D. 8, 1975, 820-828.
23. Shimizu, R., Kataoka, Y., Ikuta, T., Koshikawa, T., and Hashimoto, H. "A Monte Carlo Approach to the Direct Simulation of Electron Penetration in Solids," J. Phys. D. 9, 1976, 101-114.
24. Shimizu, R. and Everhart, T. E. "A Semiempirical Stopping Power Formula for Use in Microprobe Analysis," Appl. Phys. Lett. 33, 1978, 784-786.
25. Gryzinski, M. "Classical Theory of Atomic Collisions. I. Theory of Inelastic Collisions," Phys. Rev. 138, 1965, 336-358.
26. Adesida, I. "Electron Energy Dissipation in Layered Media," Ph.D. Dissertation, University of California, Berkeley, 1979.
27. Green, A. J. and Leckey, R. C. "Scattering of 2-20keV Electrons in Aluminum," J. Phys. D. 9, 1976, 2123-2138.
28. Shimizu, R., Aratoma, M., Ichimura, S., and Yamazaki, Y. "Application of Monte Carlo Calculation to Fundamentals of Scanning Auger Electron Microscopy," Appl. Phys. Lett. 31, 1977, 692-694.
29. Shimizu, R., "Monte Carlo Calculation in EPMA and SEM," in: Proc. 8th Int. Conf. X-Ray Optics and Microanalysis, ed. by D. Beaman, R. Ogilvie, and D. Wittry, Pendell Publ. Co., Midland, Michigan, 1980, 13-19.
30. Shimizu, R., Ichimura, S., and Aratama, M. "Application of Monte Carlo Calculation Techniques to Quantitative Analyses by AES," in: Microbeam Analysis - 1979, ed. by D. Newbury, San Francisco Press, 1979, 30-34.
31. Ichimura, S., Aratoma, M., and Shimizu, R. "Monte Carlo Calculation Approach to Quantitative AES," J. Appl. Phys. 51, 1980, 2853-2860.
32. Yamazaki, Y. "Studies on Electron Scattering by Mercury Atoms and Electron Spin Polarization Detector," Ph.D. Thesis, Osaka University, 1977.

33. Kotera, M., Murata, K., and Nagami, K. "Monte Carlo Simulation of 1-10keV Electrons in a Au Target," J. Appl. Phys. 52, 1981, 997-1003.
34. Murata, K., Kotera, M., and Nagami, K. "Remarks on the Calculation of Energy Loss in Electron-Resist Films on Substrates," Jap. J. Appl. Phys. 17, 1978, 1671-1672.
35. Murata, K., Kotera, M., and Nagami, K. "Monte Carlo Simulation of Electron Scattering at 1-10keV and its Application to Thin Film Analysis," in: Ref. 30, 35-38.
36. Spencer, L. V. and Fano, U. "Energy Spectrum Resulting From Electron Slowing Down," Phys. Rev. 93, 1954, 1172-1181.
37. Kanaya, K. and Okayama, S. "Penetration and Energy Loss Theory of Electrons in Solid Targets," J. Phys. D 5, 1972, 43-58.
38. Murata, K., Kyser, D. F., and Ting, C. H. "Monte Carlo Simulation of Fast Secondary Electron Production in Electron Beam Resists," J. Appl. Phys. 52, 1981, 4396 - 4405.
39. Moller, C. "Zur Theorie der Durchgangs Schneller Elektronen durch Materie," Ann. der Physik 14, 1932, 531-585.
40. Newbury, D. E., Mykelbust, R. L., and Heinrich, K. F. "A Hybrid Monte Carlo Procedure Employing Single and Multiple Scattering," in: Ref. 29, 57-62.
41. Newbury, D. E. and Yakowitz, H. "Studies of the Distribution of Signals in the SEM/EPMA by Monte Carlo Electron Trajectory Calculations," in: Ref. 17, 15-44.
42. Shimizu, R. "Some Recent Developments in Microbeam Analysis in Japan - Parts I and II," Technol. Reports No. 1343 and 1344, Osaka University, 1976.
43. Newbury, D. E., Yakowitz, H., and Mykelbust, R. L. "Monte Carlo Calculations of Magnetic Contrast From Cubic Materials in the SEM," Appl. Phys. Lett. 23, 1973, 488-490.
44. Ikuta, T. and Shimizu, R. "Magnetic Domain Contrast From Ferromagnetic Materials in the SEM," Phys. Stat. Sol. 23, 1974, 605-613.
45. Ikuta, T., Sugata, E., and Shimizu, R. "A Study of Type-II Magnetic Contrast by Monte Carlo Simulation," in: Microbeam Analysis - 1980, ed. by D. Wittry, San Francisco Press, 1980, 161-164.
46. Kyser, D. F. and Geiss, R. H. "Spatial Resolution of X-Ray Microanalysis in STEM," in: Proc. 12th Ann. Conf. Microbeam Analysis Society, available from San Francisco Press, 1977, paper 110.
47. Newbury, D. E. and Myklebust, R. L. "Monte Carlo Electron Trajectory Simulation of Beam Spreading in Thin Foil Targets," Ultramicroscopy 3, 1979, 391-395.
48. Geiss, R. H., and Kyser, D. F. "Thin Film X-ray Spectrometry," Ultramicroscopy 3, 1979, 397-400.
49. Kyser, D. F. Introduction to Analytical Electron Microscopy, ed. by J. Hren, J. Goldstein, and D. Joy, Plenum, New York, 1979, Ch. 6.
50. Yakowitz, H., Newbury, D. E., and Mykelbust, R. L. "Approaches to Particulate Analysis in the SEM With the Aid of a Monte Carlo Program," Scanning Electron Microsc. 1975, 93-102.
51. Newbury, D. E., Myklebust, R. L., Heinrich, K. F., and Small, J. A. "Monte Carlo Electron Trajectory Simulation - An Aid for Particle Analysis," in: Characterization of Particles, ed. by K. Heinrich, National Bureau of Standards, Spec. Publ. 533, Washington, D.C. 20234, 1980, 39-62.
52. Cvikevitch, S. and Pihl, C. "Application of Monte Carlo Simulation to Quantitative Electron Microprobe Analysis of Refractory Thin Films," in: Ref. 30, 39-42.
53. Cvikevitch, S. and Pihl, C. "Monte Carlo Simulation Applied to Electron Microprobe Thickness Measurement of Pb-Sn Oxide Films," in: Ref. 30, 39-42.
54. Pihl, C. and Cvikevitch, S. "Monte Carlo Simulation Approach to Quantitative Electron Microprobe Analysis of Ternary Alloy Thin Films," in: Ref. 45, 157-160.
55. Reuter, W., Kuptsis, J. D., Lurio, A., and Kyser, D. F. "X-Ray Production Range in Solids by 2-15keV Electrons," J. Phys. D. 11, 1978, 2633-2642.
56. Love, G., Cox, M. G., and Scott, V. D. "A Simple Monte Carlo Method for Simulating Electron-Solid Interactions and its Application to Electron Probe Microanalysis," J. Phys. D 10, 1977, 7-23.
57. Love, G., Cox, M. G., and Scott, V. D. "A Versatile Atomic Number Correction for Electron Probe Microanalysis," J. Phys. D 11, 1978, 7-21.
58. Love, G., Cox, M. G., and Scott, V. D. "The Surface Ionization Function Derived Using a Monte Carlo Method," J. Phys. D 11, 1978, 23-31.
59. Kyser, D. F. and Murata, K. "Monte Carlo Simulation of Electron Beam Scattering and Energy Loss in Thin Films on Thick Substrates," in: Proc. 6th Int. Conf. Electron and Ion beam Science and Technology, ed. by R. Bakish, Electrochemical Society, Princeton, New Jersey, 1974, 205-223.
60. Hawryluk, D. J., Hawryluk, A. M., and Smith, H. I. Energy Dissipation in a Thin Polymer Film by Electron Beam Scattering," J. Appl. Phys. 45, 1974, 2551-2566.
61. Parikh, M. "Corrections for Proximity Effects in Electron Beam Lithography, Parts I, II, and III," J. Appl. Phys. 50, 1979, 4371-4387.
62. Parikh, M. and Kyser, D. F. "Energy Deposition Functions in Electron Resist Films on Substrates," J. Appl. Phys. 50, 1979, 1104-1111.
63. Kyser, D. F. and Pyle, R. "Computer Simulation of Electron Beam Resist Profiles," IBM J. Res. Develop. 24, 1980, 426-437.
64. Lin, Yi-C. "Alignment Signals From Electrons Scattering Near an Edge for Electron Beam Microfabrication," Ph.D. Dissertation, University of California, Berkeley, 1981.
65. Neureuther, A. R., Kyser, D. F., and Ting, C. H. "Electron-Beam Resist Edge Profile Simulation," IEEE Trans. Electron Devices ED-26, 1979, 686-693.
66. Stephani, D. "Ein Beitrag zur Automatischen Markenerkennung in der Elektronenstrahl-Lithographie," Ph.D. Thesis, Technical University of Aachen, 1981.
67. Adesida, I., Shimizu, R., and Everhart, T. "A Study of Electron Penetration in Solids Using a Direct Monte Carlo Approach," J. Appl. Phys. 51, 1980, 5962-5969.
68. Adesida, I. and Everhart, T. "Substrate Thickness Considerations in Electron Beam Lithography," J. Appl. Phys. 51, 1980, 5994-6005.

69. Shimizu, R. "Practicality of Monte Carlo Technique for Quantitative Microanalysis," in: Ref. 19, 156-218.
70. Hawryluk, R. J. and Hawryluk, A. M. "Computer Code Used in Monte Carlo Calculations," MIT Lincon Lab, Lexington, MA, Technical Note 1974-51, 1974.
71. Niedrig, H. "Backscattered Electrons as a Tool for Film Thickness Determination," Scanning Electron Microsc. 1978:I, 841-858.
72. Kyser, D. F. and Viswanathan, N. S. "Monte Carlo Simulation of Spatially Distributed Beams in Electron Beam Lithography," J. Vac. Sci. Technol. 12, 1975, 1305-1308.
73. Ishitani, T., Shimizu, R., and Murata, K. "Monte Carlo Simulations on Scattering of Bombarded Ions in Solids," Jap. J. Appl. Phys. 11, 1972, 125-133.
74. Ishitani, T., Shimizu, R., and Murata, K. "Monte Carlo Simulations of the Behavior of Energetic Ions in Polyatomic Targets," Phys. Stat. Sol. 50, 1972, 681-690.
75. Ishitani, T. Shimizu, R. "Computer Simulation of Atomic Mixing During Ion Bombardment," Appl. Phys. 6, 1975, 241-248.
76. Kang, S., Shimizu, R., and Okutani, T. "Sputtering of Si With keV $Ar^+$ Ions - Part I," Jap. J. Appl. Phys. 18, 1979, 1717-1725.
77. Kang, S., Shimizu, R., and Okutani, T. "Sputtering of Si With keV $Ar^+$ Ions - Part II," Jap. J. Appl. Phys. 18, 1979, 1987-1994.
78. Biersack, J. P. and Haggmark, L. G. "A Monte Carlo Computer Program for the Transport of Energetic Ions in Amorphous Targets," Nuclear Inst. and Methods 174, 1980, 257.

## Discussion with Reviewers

H. Niedrig: You quote the work of Reimer and Krefting, who showed that by utilizing the more exact Mott elastic scattering cross-section in Monte Carlo calculations, better agreement with experimental results for backscattered and transmitted electrons is obtained, especially for films of high atomic number. On the other hand, Fathers and Rez (Scanning Electron Microsc./1979:I; p. 55) stated that from their transport equation calculations for backscattering from bulk solids, "the details of the cross-section for very small or very large angles is relatively unimportant." Could you comment on this? Is there a discrepancy, or does the higher Mott cross-section for wide angle scattering mainly affect the backscattering from films and not so much from bulk solids?

Author: The conclusion of Fathers and Rez is not necessarily in quantitative disagreement with the view of Reimer and Krefting, since Fathers and Rez make only a qualitative statement about the role of scattering cross-section details upon the backscatter yield from bulk targets.

One of the most severe tests of any scattering theory is that of comparing results on transmitted and backscattered electrons for thin foil targets and for a wide range of foil thickness. If the Mott cross-section is justified in the present applications, then Figure 6 shows that the dynamic range of cross-section with small and large scattering angles should be important, especially for high Z targets. For very thin foils, where only a few scattering events can occur, the details of the scattering cross-section are very important. It would be very interesting to calculate the electron transmission and backscatter yields and categorize the results with restricted ranges of scattering angles along each trajectory. Such calculations are easily accomplished with Monte Carlo methods for trajectory simulation, and we believe the Monte Carlo method is more tractable and offers more insight into the physics of electron scattering than any other method.

D.E. Newbury: When implementing one of the Monte Carlo programs available in the literature, a user would be wise to test the calculated results with experimental data to ascertain that the calculation is in fact doing what it should do. Can you recommend a logical series of comparisons against experimental data with which a novice to the field could test a new Monte Carlo program?

Author: In the opinion and experience of the author, a great deal of confidence in a new Monte Carlo program can be gained by simply observing some of the electron trajectories on a plotter or video display terminal such as those presented in Figure 4. Any wild deviations or aberrations will be apparent immediately. After that, a series of quantitative tests can be made with the following theoretical and experimental data:

1. depth distribution of energy deposition ($dE/dz$) and X-ray production $\phi(\rho z)$.
2. dependence of electron backscatter number yield ($\eta$) upon target atomic number (Z), beam voltage ($E_0$), and incidence angle ($\theta$).
3. energy and angular distribution of backscattered electrons.
4. energy and angular distribution of transmitted electrons.
5. quantitative electron probe microanalysis of known compounds.

When making such comparisons, one must keep in mind that any experimental result has an associated error, and some experimental results may differ with other results. Hence the comparison must be made very carefully when looking for details. Some Monte Carlo programs may be designed for particular target configurations such as thin films on substrates, particles, discontinuous media, stepped surfaces, etc. It is just such difficult boundary conditions as these which can only be treated accurately with Monte Carlo simulation of electron scattering. However, the input data which describes the target geometry can usually be set to some limit such that the calculated results can be compared with the experimental data which is usually obtained from simpler targets such as semi-infinite, flat, or continuous media.

Additional discussion with reviewers of the paper "Monte Carlo Calculations for Electron Microscopy, Microanalysis, and Microlithography".

D. E. Newbury: Deep in the heart of nearly every Monte Carlo technique is an "adjustable parameter" which must be chosen to give a good match between a calculated result and the trusted experimental value, e.g., backscatter yield. Can you describe a procedure for selecting these adjustable parameters and comment on the physical reality (or lack thereof) of these parameters? Usually the parameter is a multiplier on the step length.

Author: It is certainly true that some Monte Carlo models contain some form of "adjustable parameter" to provide a systematic correction to some variable (such as step length $\Lambda$ or screening parameter $\beta$) which results in the best agreement with experimental data on some arbitrary signal such as $\eta$, $\phi(\rho z)$, etc. However, the correction is usually very small, and simply represents a lack of full theoretical knowledge about the various components of the model which comprise a complete Monte Carlo simulation of electron scattering and energy loss. Or the "adjustable parameter" may be required because of some approximations made to minimize the computational time or some other practical limitation. This does not invalidate the use of the technique for important applications, but does represent a challenge to the theoretical physicists and applied mathematicians who are concerned about the purity and fundamental nature of the method.

H. E. Bishop: (1) I have always found Reference 1 most helpful as an introduction to the practical aspects of Monte Carlo calculations. I would strongly recommend everyone reading it before preparation of any computer program. (2) The paper by F. James, "Monte Carlo in Theory and Practice," Rep. Prog. Phys. 43, 1145 (1980) gives a formal discussion of the mathematical basis of the Monte Carlo approach and also contains a useful discussion on random numbers. (3) The improvement in accuracy of the "single scattering" model over the full "multiple scattering" approach is due to the shorter step length. From the computational point of view, the single scattering approach has the additional advantage that the scattering angle can be calculated from Eq. (9) rather than having to store tables of multiple scattering distributions for each energy step. (4) The comment about the convergence of Eq. (4) is not necessarily true. If the equation is recast to exclude the unscattered portion of the distribution (see References 3 and 21), then there is no great problem with convergence, certainly for energies below 30 keV. (5) As a rule of thumb, the screened Rutherford cross-section gives reasonable results above the K ionization energy of the elements involved.

Author: I want to thank this reviewer for these helpful comments, and especially for the reference to the recent paper by James of which we were not aware.

H. E. Bishop: As many Monte Carlo calculations are now made for the TEM, should relativistic effects be included in the theory?

Author: Yes, the relativistic electron effects should be included in the scattering and energy loss equations for such high energies.

H. E. Bishop: Why do the partial wave solutions in Figure 6 deviate from the screened Rutherford cross-section at small angles?

Author: The method of partial wave expansion for calculation of elastic scattering cross-sections is very complex, and is beyond the intent of the present paper. A detailed description of the method can be found in Reference 32, as well as a description of the relativistic Rutherford scattering formula. Basically, the partial wave method includes the phase shift of the scattered electron.

R. B. Bolon: Would you comment on the magnitude of the effect of the production of fast secondary electrons in regard to their relative number and the resulting effect on the magnitude and spatial distribution of characteristic X-rays? Do any Monte Carlo models consider these effects?

Author: Although each primary electron can generate a large number of secondary electrons, and the secondary electrons can generate tertiary electrons, etc., the dominant factor for characteristic X-ray production by secondary electrons is the energy distribution of the secondary electrons produced. As described in Reference 38, the scattering cross-section greatly favors the production of lower energy secondary electrons. In order to affect the production of characteristic X-rays, the fast secondary electron must be produced with an initial energy of at least the ionization energy $E_c$ of an inner shell electron. Hence the fast secondary electrons would be important to consider only for soft X-ray production ($E_c$<1 keV), and even then it is probably a negligible effect. The author is not aware of any detailed Monte Carlo calculations of secondary electron effects on characteristic X-ray production, although the Monte Carlo model of Reference 38 could be used to investigate the magnitude of the effect.